

Supporting Information

**The interface hydrophilic-hydrophobic integration of
fluorinated defective graphene towards biomedical
applications**

Jiawen Wang,^{a,b} Yi Yu,^b Huilong Dong,^c Yujin Ji,^b Weihua Ning,^{*b}

Youyong Li^{*a,b}

- a. Macao Institute of Materials Science and Engineering, Macau University of Science and Technology, Taipa 999078, Macau SAR, China
- b. Institute of Functional Nano & Soft Materials (FUNSOM), Soochow University, Suzhou, Jiangsu 215123, China
- c. School of Materials Engineering, Changshu Institute of Technology, Changshu, Jiangsu 215500, China

* Corresponding authors. Email: yyli@suda.edu.cn, whning@suda.edu.cn

Section 1 Methods

1. Setups of different systems

Table S1. The information for molecular dynamic simulation systems.

Simulation systems	Box size (nm³)	Total atom number	Simulation Time (ns)	Number of simulations
DG-RBD	15.6*14.1*10.2	218978	500	3
FDG-RBD	15.6*14.1*10.2	218355	500	3
DG-M^{pro}	16.2*14.3*7.13	167044	500	3
FDG-M^{pro}	16.2*14.3*7.13	166463	500	3
FDG-F3-R4-K5	15.7*13.8*5.4	111345	20	1
DG-dAMP	15.7*13.8*5.4	112151	50	5
FDG-dAMP	15.7*13.8*5.4	111366	50	5
DG-dTMP	15.7*13.8*5.4	112154	50	5
FDG-dTMP	15.7*13.8*5.4	111360	50	5
DG-dCMP	15.7*13.8*5.4	112164	50	5
FDG-dCMP	15.7*13.8*5.4	111358	50	5
DG-dGMP	15.7*13.8*5.4	112158	50	5
FDG-dGMP	15.7*13.8*5.4	111367	50	5

2. Modeling of DG and FDG

The modeling of DG and FDG is done by the following steps: **1)** Utilizing the Atomic Simulation Environment (ASE) software package, we constructed an intact graphene, which contains approximately 5400 C atoms. **2)** Randomly remove C atoms according to a 5% ratio using Python's randomness principles. **3)** Import graphene nanosheets with random distribution into the Materials Studio software. Materials Studio will automatically identify which C atoms are in an unsaturated state. Subsequently, these unsaturated C atoms will undergo oxidation treatment by oxidizing groups (bridge oxygen (-O-), hydroxyl (-OH), fewer carboxyl (-COO⁻), and carbonyl (=O)), resulting in defective graphene (DG). **4)** On the basis of the defective graphene, we fluorinated the area around the oxygen-containing defect with a fluoridation rate of 15%, and finally obtained the fluorinated defective graphene (FDG). Finally, these two types of graphene nanosheets share the same length and width, which are 13.39 nm * 11.54 nm, respectively.

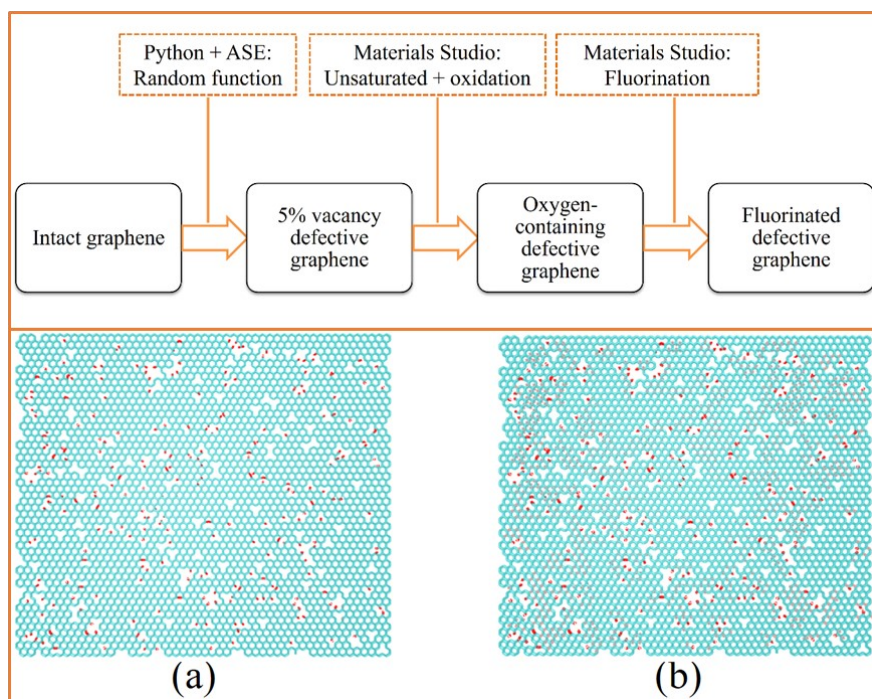


Fig. S1. Atomic structures of (a) DG and (b) FDG. Investigated materials highlighted by “Lines” drawing methods. The C, O, H and F atoms of investigated materials are represented by cyan, red, white and pink balls, respectively.

3. Diagram of the five initial positions of deoxynucleotides relative to investigated materials

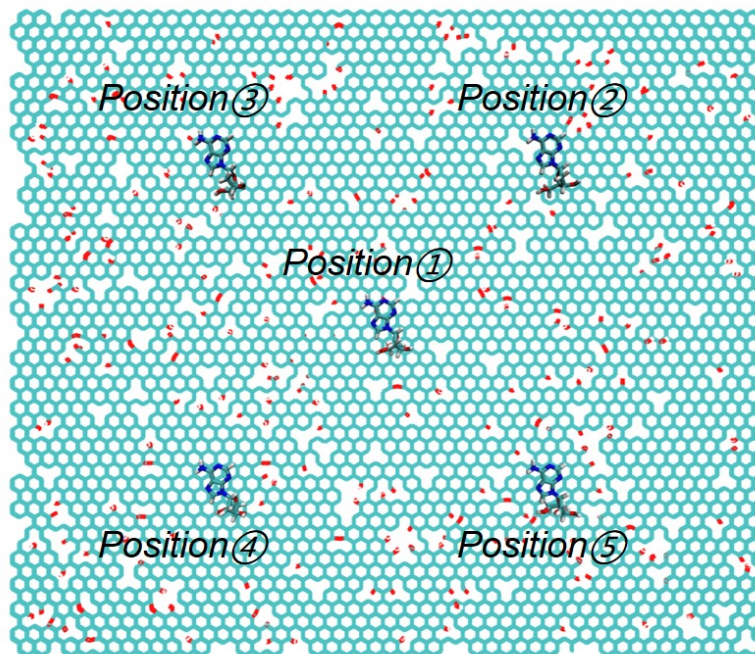


Fig. S2. Diagram of five initial positions of deoxynucleotides relative to investigated materials. Investigated materials highlighted by “Lines” drawing methods. The C, O, H and F atoms of investigated materials are represented by cyan, red, white and pink balls, respectively.

4. Data analysis

Here are some details of the data analysis:

The centroid of protein is defined as the geometric center of protein.

The interaction energy is calculated using the VMD plugin (NAMD energy), with the interaction energy = van der Waals energy + electrostatic energy.

The contact area is calculated as: $\text{Contact area} = 1/2(\text{SAS}_{\text{protein}} + \text{SAS}_{\text{(investigated material)}} - \text{SAS}_{\text{(protein-investigated material complex)}})$, where $\text{SAS}_{\text{protein}}$ and $\text{SAS}_{\text{(investigated material)}}$ are the solvent accessible surface (SAS) area of the isolated protein and investigated material, respectively, and $\text{SAS}_{\text{(protein-investigated material complex)}}$ is that of the protein-investigated material complex¹. The solvent radius is set to 1.4 Å.

Amino acids within 6 Å of the investigated material's surface are defined as being in contact.

In Table 2, the moving range represents the area within which a single deoxynucleotide moves on the investigated material, calculated using the convex hull algorithm.

Section 2 Result and discussion

5. Other independent simulation for RDB-DG systems

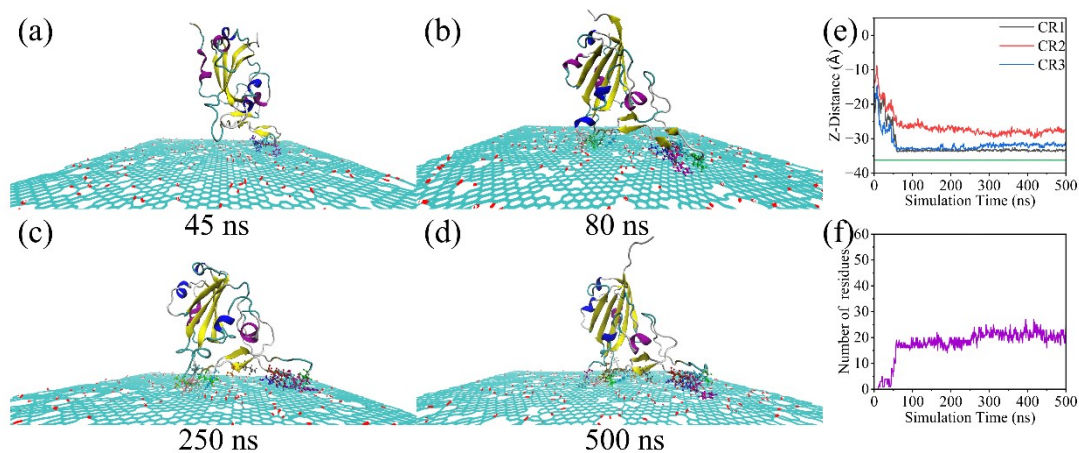


Fig. S3. (a-d) Representative trajectory snapshots of RBD adsorbed onto DG (**Trajectory2**). RBD and investigated materials highlighted by “Newcartoon” and “Lines” drawing methods. Amino acids in contact with the surface highlighted by “CPK” drawing method. (e) Z-direction centroid distance of CR1-CR3. The green lines represent the Z-direction centroid distance of DG. (f) The number of residues in contact with the DG.

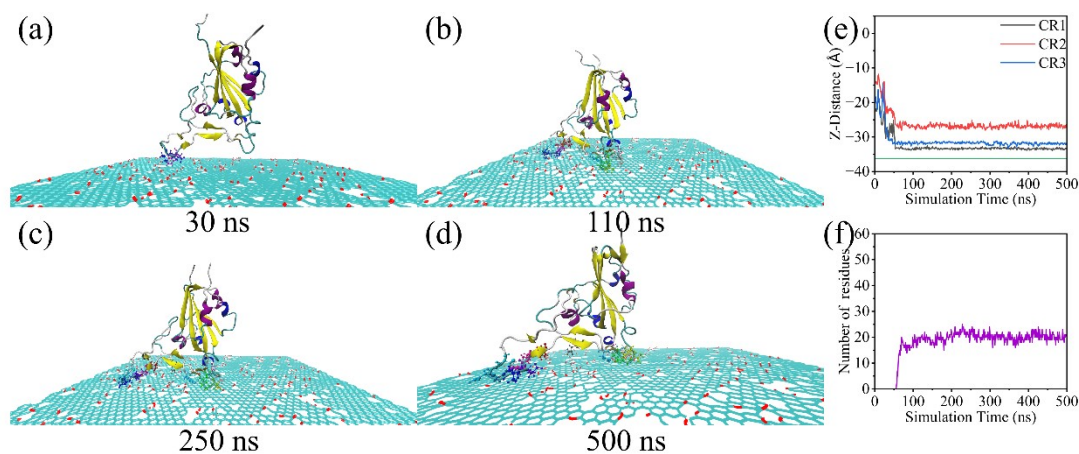


Fig. S4. (a-d) Representative trajectory snapshots of RBD adsorbed onto DG (**Trajectory3**). RBD and investigated materials highlighted by “Newcartoon” and “Lines” drawing methods. Amino acids in contact with the surface highlighted by “CPK” drawing method. (e) Z-direction centroid distance of CR1-CR3. The green lines

represent the Z-direction centroid distance of DG. (f) The number of residues in contact with the DG.

6. Other independent simulation for RBD-FDG systems

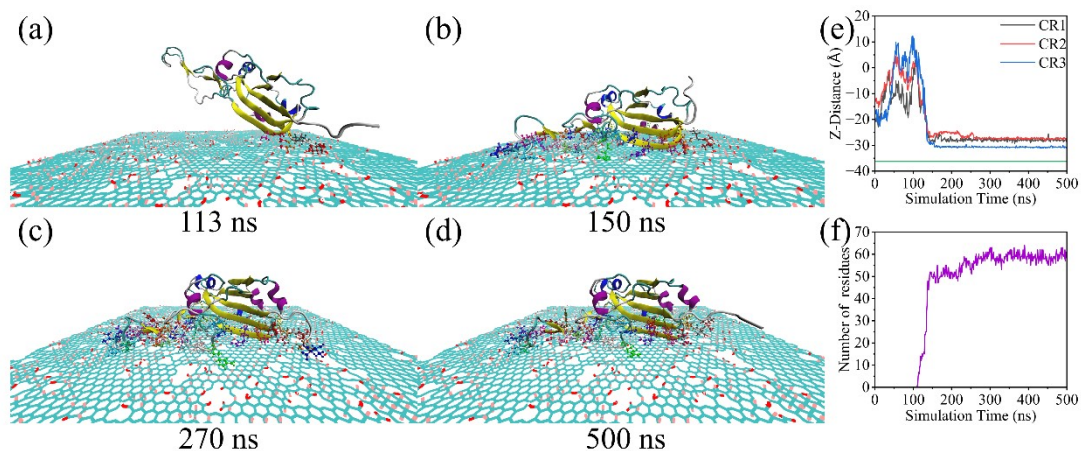


Fig. S5. (a-d) Representative trajectory snapshots of RBD adsorbed onto FDG (**Trajectory2**). RBD and investigated materials highlighted by “Newcartoon” and “Lines” drawing methods. Amino acids in contact with the surface highlighted by “CPK” drawing method. (e) Z-direction centroid distance of CR1-CR3. The green lines represent the Z-direction centroid distance of FDG. (f) The number of residues in contact with the FDG.

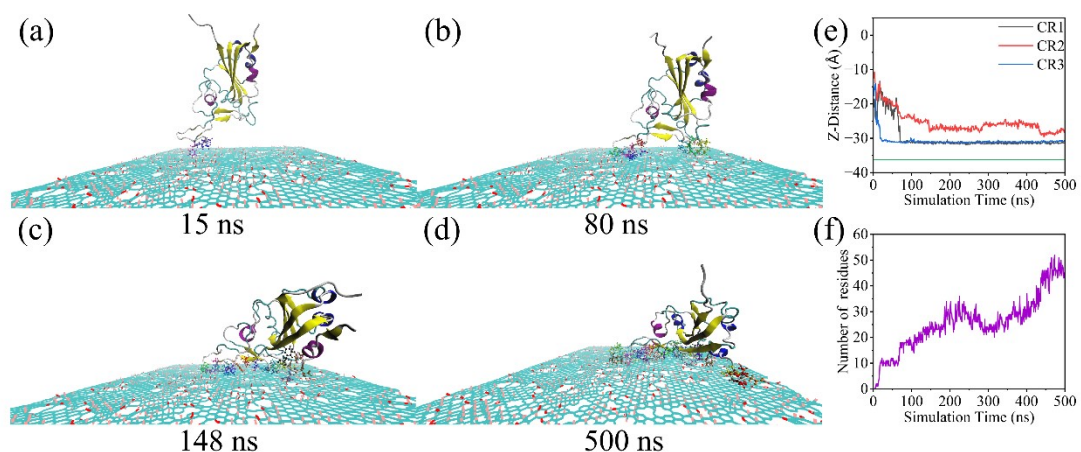


Fig. S6. (a-d) Representative trajectory snapshots of RBD adsorbed onto FDG (**Trajectory3**). RBD and investigated materials highlighted by “Newcartoon” and “Lines” drawing methods. Amino acids in contact with the surface highlighted by “CPK” drawing method. (e) Z-direction centroid distance of CR1-CR3. The green lines represent the Z-direction centroid distance of FDG. (f) The number of residues in contact with the FDG.

7. Other independent simulation for M^{pro}-DG MD systems

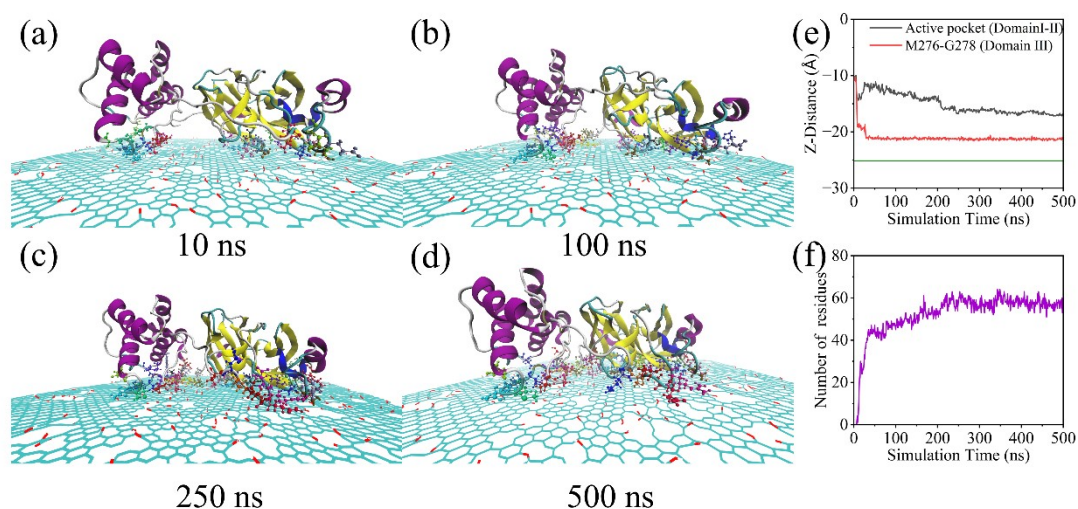


Fig. S7. Representative trajectory snapshots of M^{pro} adsorbed onto DG (**Trajectory2**). M^{pro} and investigated materials highlighted by “Newcartoon” and “Lines” drawing methods. Amino acids in contact with the surface highlighted by “CPK” drawing method. (e) Z-direction centroid distance of M276-G278 (Domain III) and Active pocket (Domain I-II). The green lines represent the Z-direction centroid distance of DG. (f) The number of residues in contact with the DG.

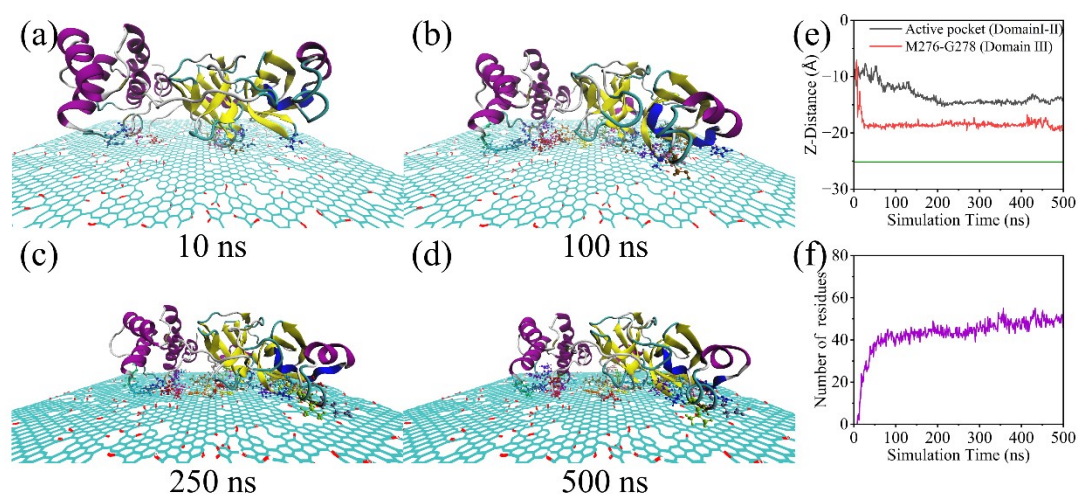


Fig. S8. Representative trajectory snapshots of M^{pro} adsorbed onto DG (**Trajectory3**). M^{pro} and investigated materials highlighted by “Newcartoon” and “Lines” drawing methods. Amino acids in contact with the surface highlighted by “CPK” drawing method. (e) Z-direction centroid distance of M276-G278 (Domain III) and Active S10

pocket (Domain I-II). The green lines represent the Z-direction centroid distance of DG.

(f) The number of residues in contact with the DG.

8. Other independent simulation for M^{pro}-FDG MD systems

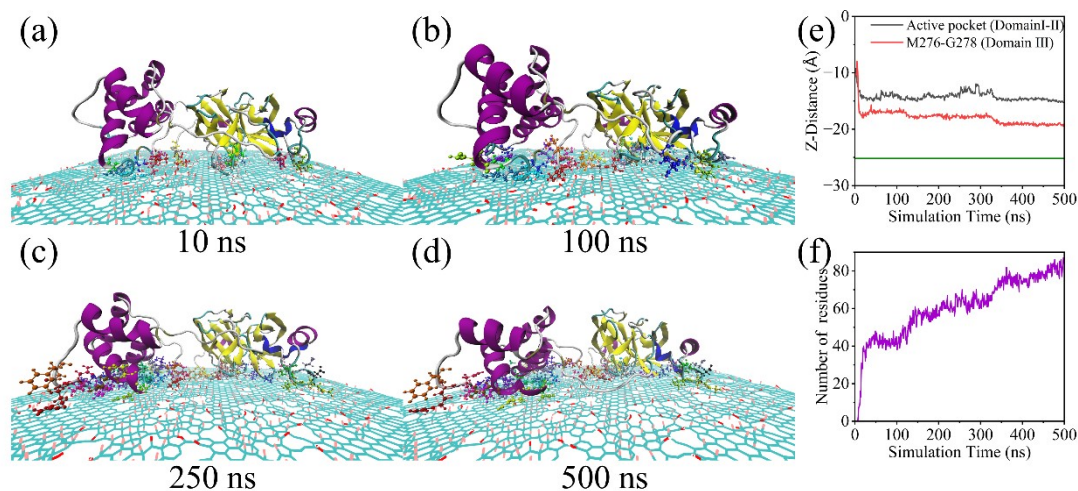


Fig. S9. Representative trajectory snapshots of M^{pro} adsorbed onto FDG (**Trajectory2**). M^{pro} and investigated materials highlighted by “Newcartoon” and “Lines” drawing methods. Amino acids in contact with the surface highlighted by “CPK” drawing method. (e) Z-direction centroid distance of M276-G278 (Domain III) and Active pocket (Domain I-II). The green lines represent the Z-direction centroid distance of FDG. (f) The number of residues in contact with the FDG.

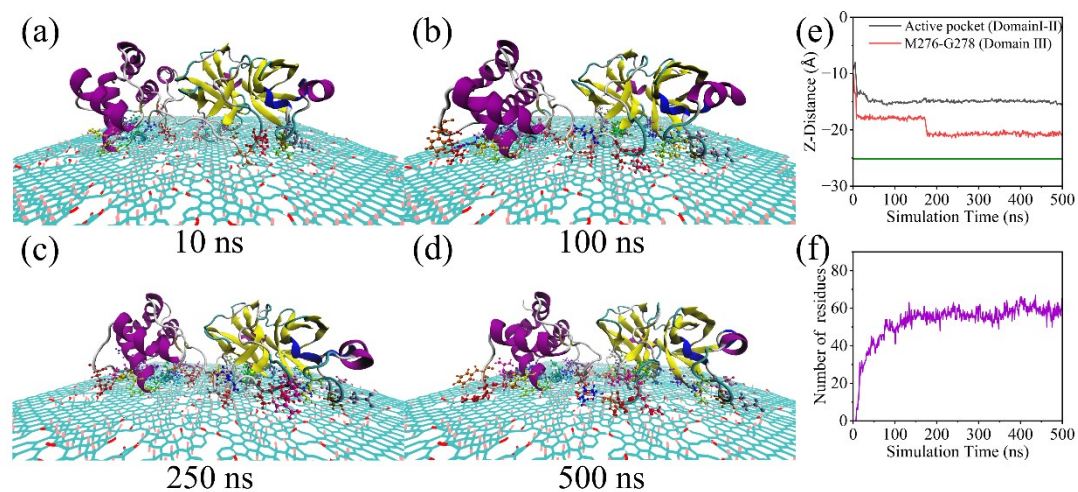


Fig. S10. Representative trajectory snapshots of M^{pro} adsorbed onto FDG (**Trajectory3**). M^{pro} and investigated materials highlighted by “Newcartoon” and “Lines” drawing methods. Amino acids in contact with the surface highlighted by “CPK” drawing method. (e) Z-direction centroid distance of M276-G278 (Domain III)

and Active pocket (Domain I-II). The green lines represent the Z-direction centroid distance of FDG. (f) The number of residues in contact with the FDG.

9. The centroid migration path for other RBD-DG/FDG MD simulation systems

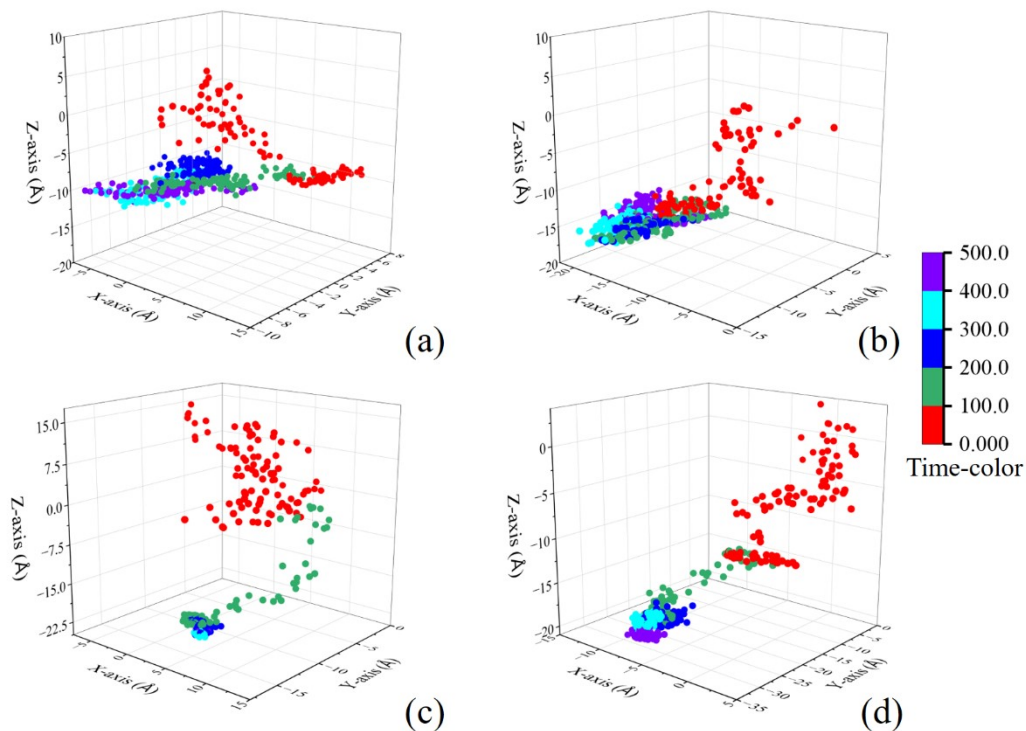


Fig. S11. Representative centroid migration path of RBD on the (a-b) DG and (c-d) FDG during 500 ns. The corresponding Z-axis coordinates of investigated materials is approximately -36.5 Å.

10.The centroid migration path for other M^{pro}-DG/FDG MD simulation systems

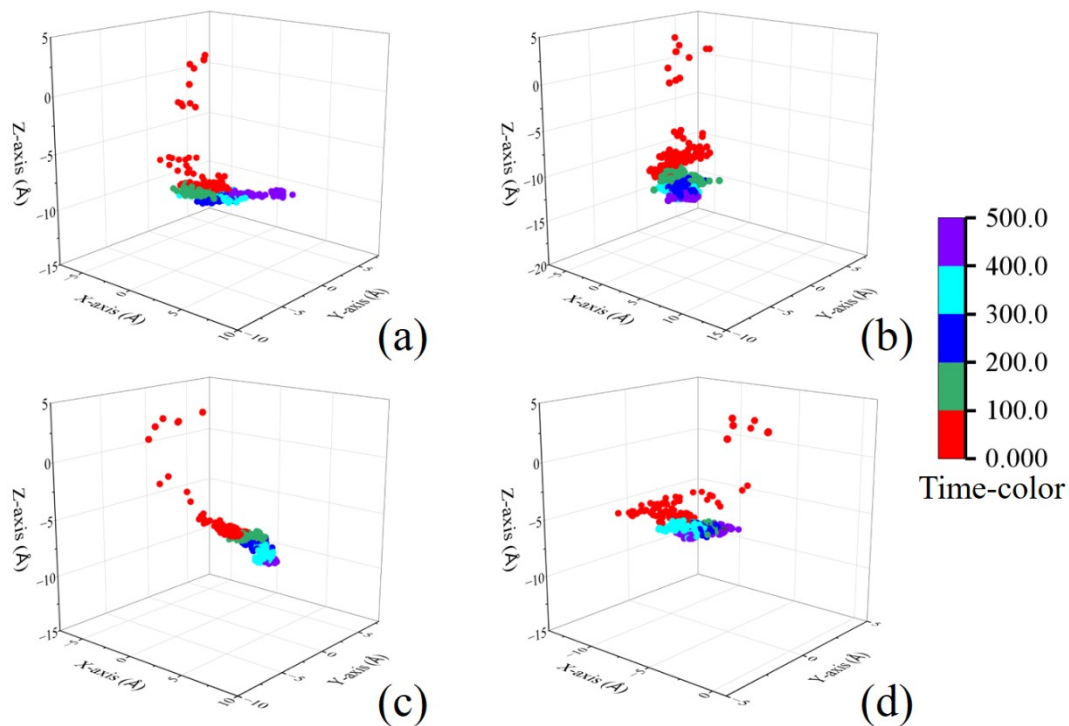


Fig. S12. Representative centroid migration path of M^{pro} on the (a-b) DG and (c-d) FDG during 500 ns. The corresponding Z-axis coordinates of investigated materials is approximately -24.5 Å.

11. The secondary structure of RBD for other RBD-DG/FDG MD simulation systems

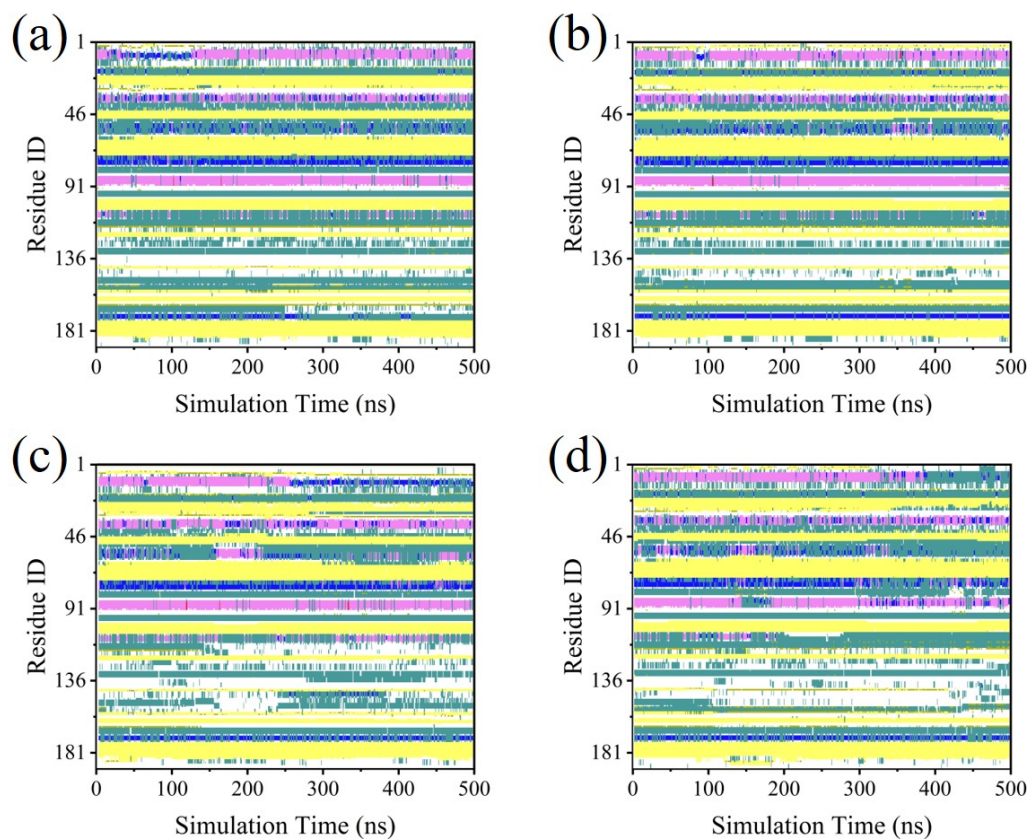


Fig. S13. Secondary structure of the RBD adsorbed on (a-b) DG and (c-d) FDG during 500 ns MD simulations. The correspondence between color and secondary structure is as follows: pink and blue represent helical structures; green represents turn structures; yellow represents sheet structures; and white represents random coil structures.

12. Other representative snapshots of the CR1-CR3 of RBD adsorbed onto DG and FDG

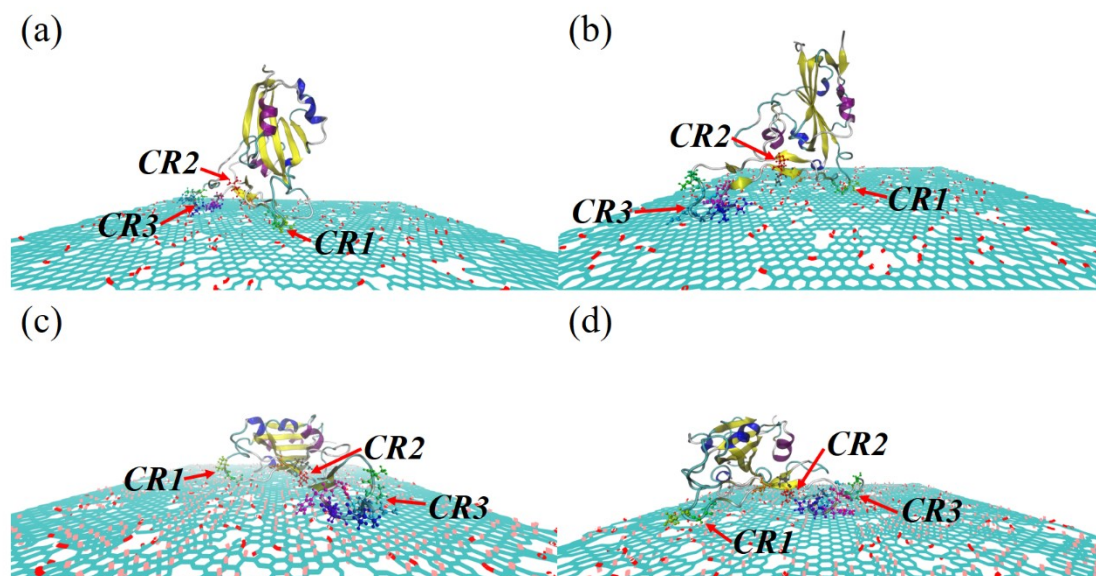


Fig. S14. At 500 ns, other representative snapshots of the CR1-CR3 (highlighted by “CPK” drawing method) of RBD adsorbed onto (a-b) DG and (c-d) FDG. Investigated materials highlighted by “Lines” drawing methods. The C, O, H and F atoms of investigated materials are represented by cyan, red, white and pink balls, respectively.

13. Other representative snapshots of the active pocket of M^{pro} adsorbed onto DG and FDG

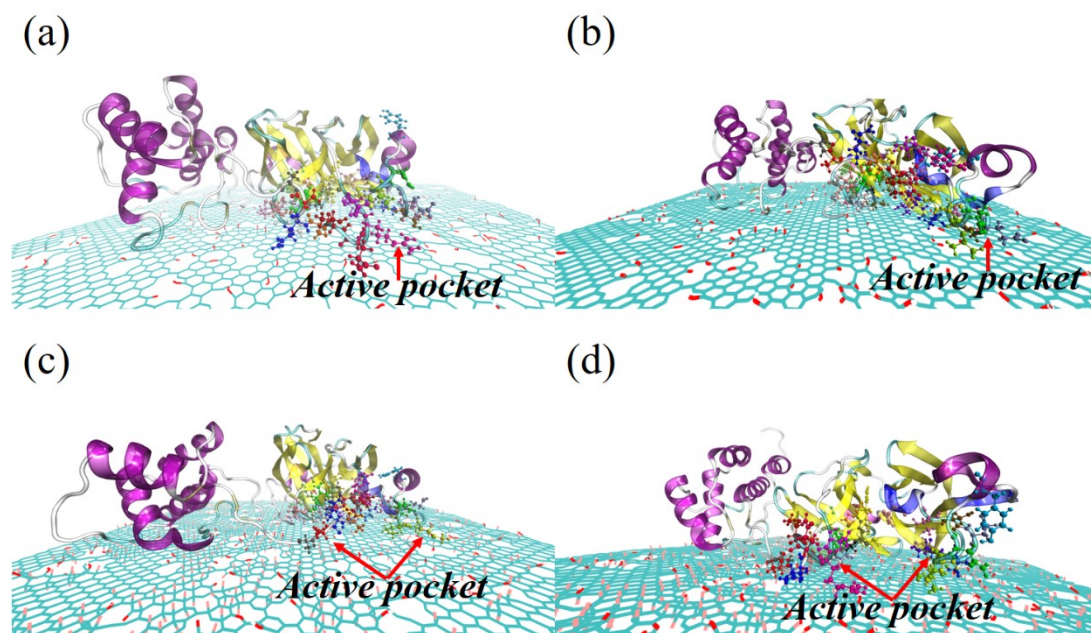


Fig. S15. At 500 ns, other representative snapshots of the active pocket (highlighted by “CPK” drawing method) of M^{pro} adsorbed onto (a-b) DG and (c-d) FDG. Investigated materials highlighted by “Lines” drawing methods. The C, O, H and F atoms of investigated materials are represented by cyan, red, white and pink balls, respectively.

14. The crystal structure of the active pocket of M^{pro}, which adsorbed onto DG and FDG.

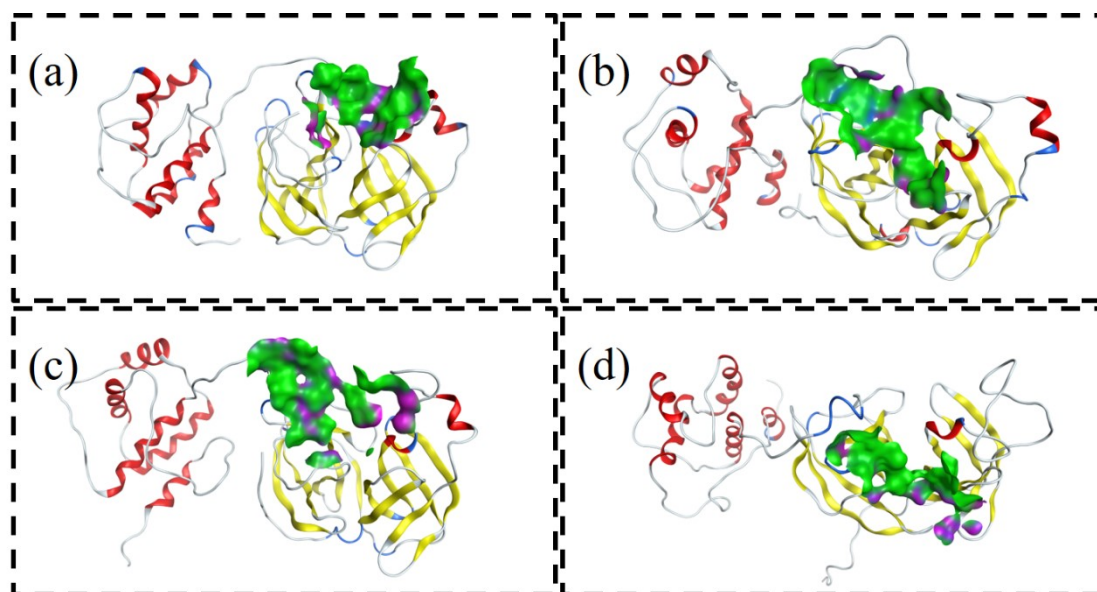


Fig. S16. The crystal structure of the active pocket compared with the active pocket of M^{pro}, which adsorbed onto (a-b) DG and (c-d) FDG. The surfaces of the active pocket use purple to represent the H-bonds region, green to represent the hydrophobic region, and blue to represent the polar region.

15. Final bound structure of M^{pro} and ligand N3 for original and the “ M^{pro} - FDG” system

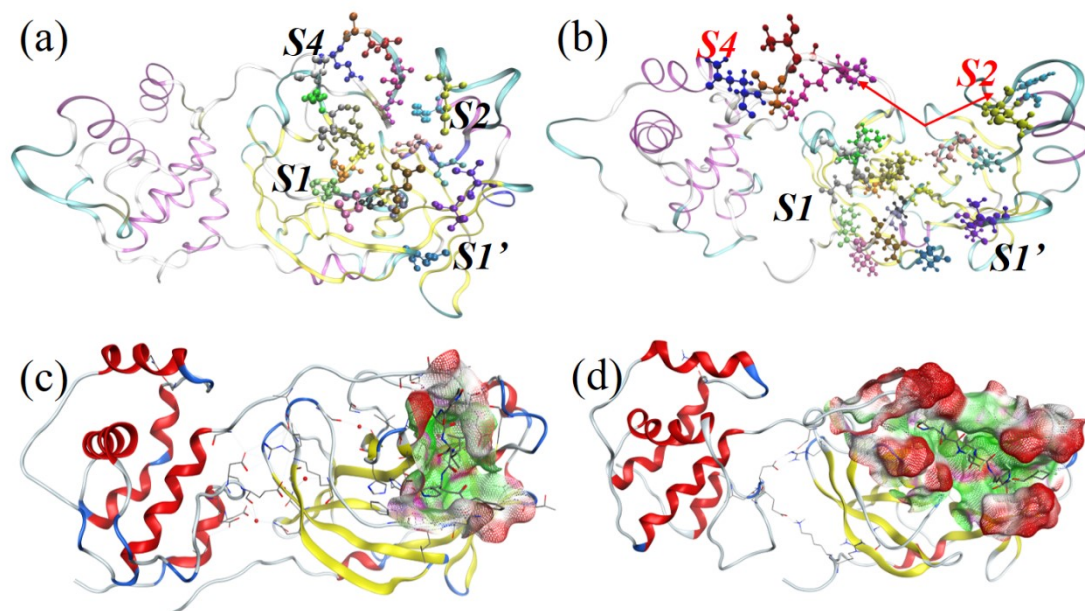


Fig. S17. Final structure of subsites for (a) “ M^{pro} -DG” and (b) “ M^{pro} -FDG” systems. Final bound structure of M^{pro} and N3 for (c) “ M^{pro} -DG” and (d) “ M^{pro} -FDG” systems. The surfaces of their binding pockets were colored by H-bond regions (red), hydrophobic regions (green), and polar regions (black). Subsites and N3 are highlighted by “CPK” and “lines” drawing methods, respectively.

Table S2. The interaction energy between the active pocket of M^{pro} and investigated materials (kcal/mol).

Simulation systems	Total energy
M^{pro} -DG	-40.09
M^{pro} -FDG	-31.94

16. The average H-bonds between water or proteins and investigated materials

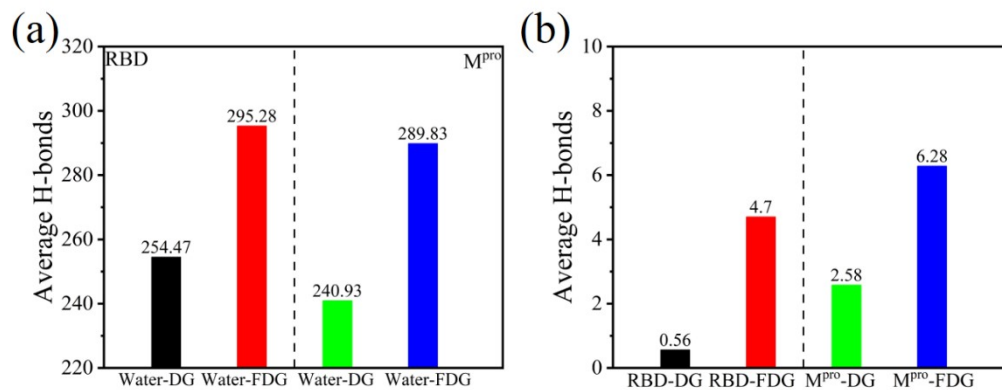


Fig. S18. (a) The average H-bonds between water and investigated materials. (b) The average H-bonds between RBD/M^{pro} and investigated materials.

17. Scan water molecules along the vertical directions in M^{pro}-DG/FDG systems

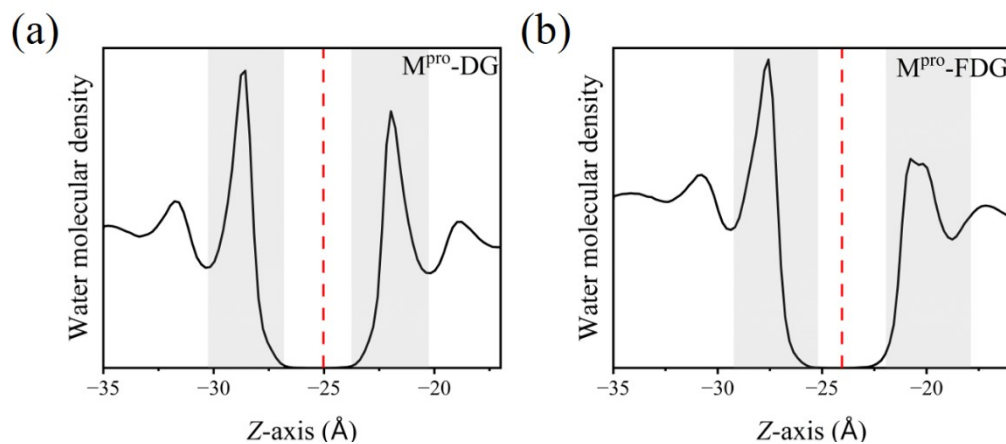


Fig. S19. Scan water molecules within the 12 Å range of (a) DG and (b) FDG along the vertical directions for M^{pro}-investigated materials systems.

18. The interactions energy decomposition between proteins and investigated materials

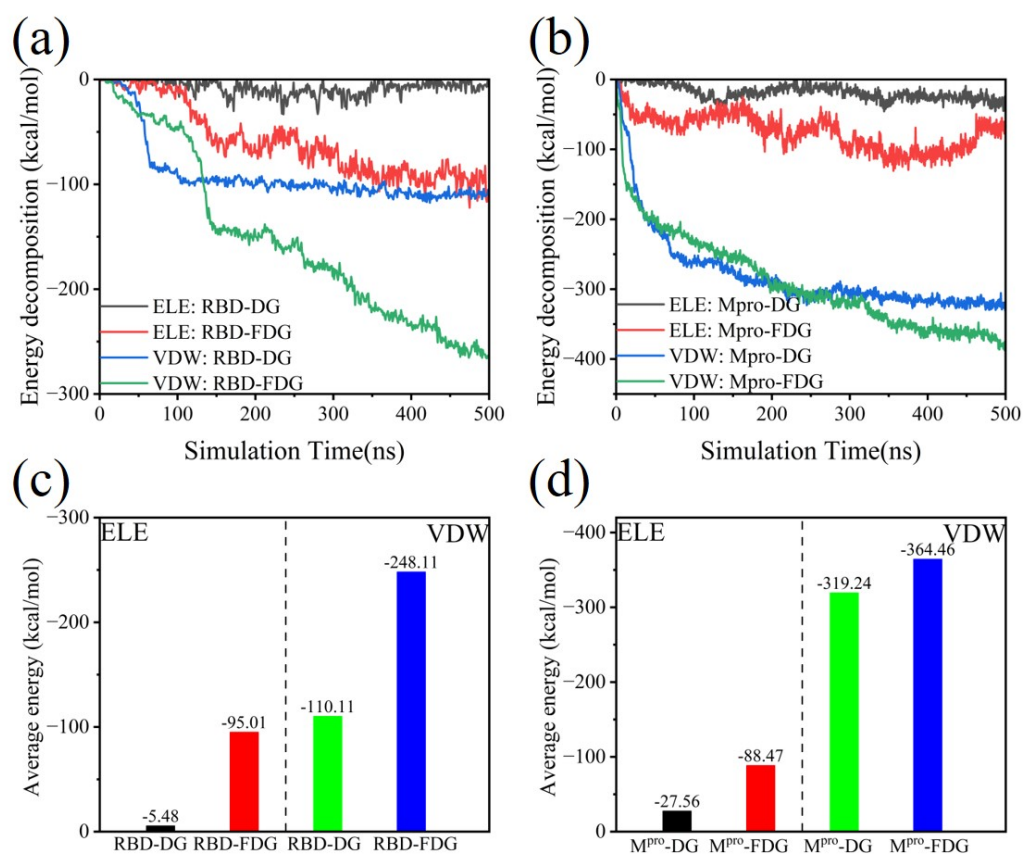


Fig. S20. The energy decomposition for (a) RBD-investigated materials and (b) M^{pro}-investigated materials systems. The average energy for (c) RBD-investigated materials and (d) M^{pro}-investigated materials systems.

19. Representative trajectory snapshots of aromatic amino acids

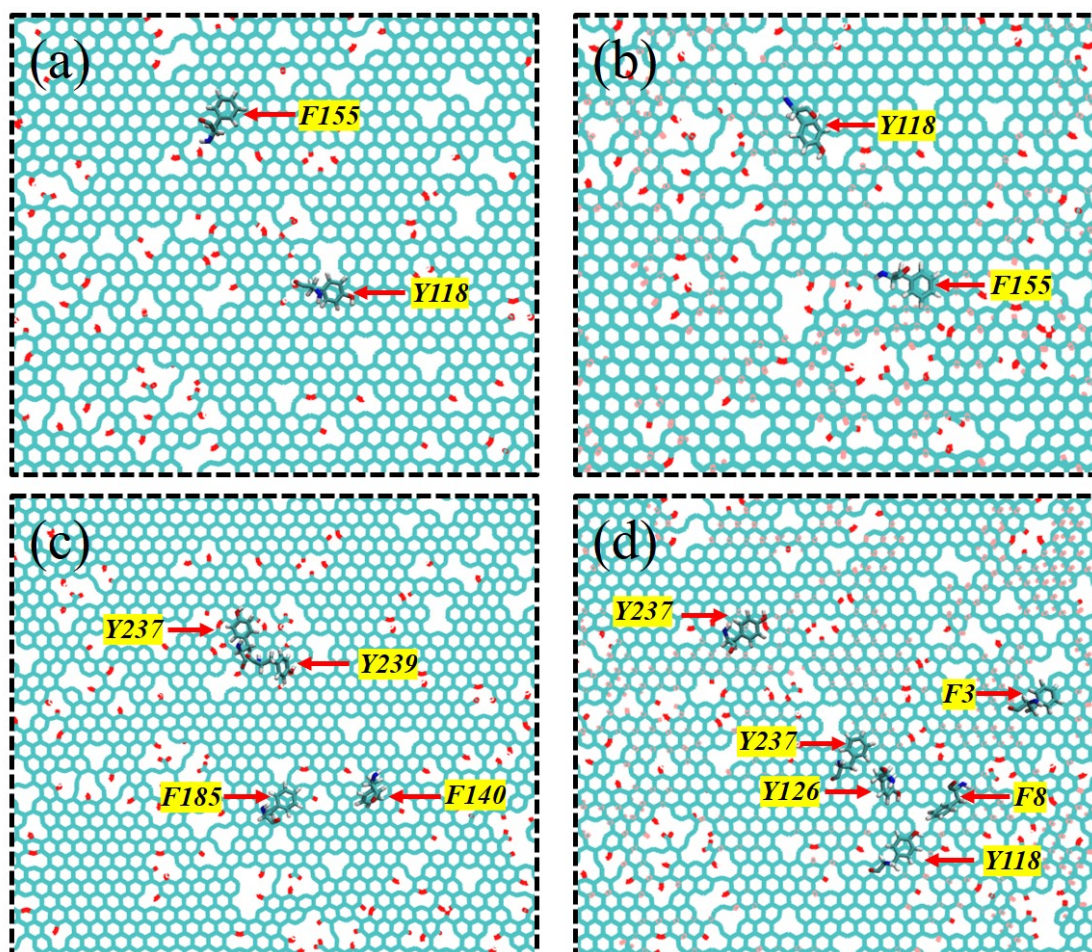


Fig. S21. From the top views, representative snapshot of some aromatic amino acids located for RBD on (a) DG and (b) FDG. From the top views, representative snapshot of some aromatic amino acids for M^{pro} located on (c) DG and (d) FDG. Aromatic amino acids and investigated materials highlighted by “Licorice” and “Lines” drawing methods. The C, O, H and F atoms of investigated materials are represented by cyan, red, white and pink balls, respectively.

20. Hedgehog plot and DCCM of RBD

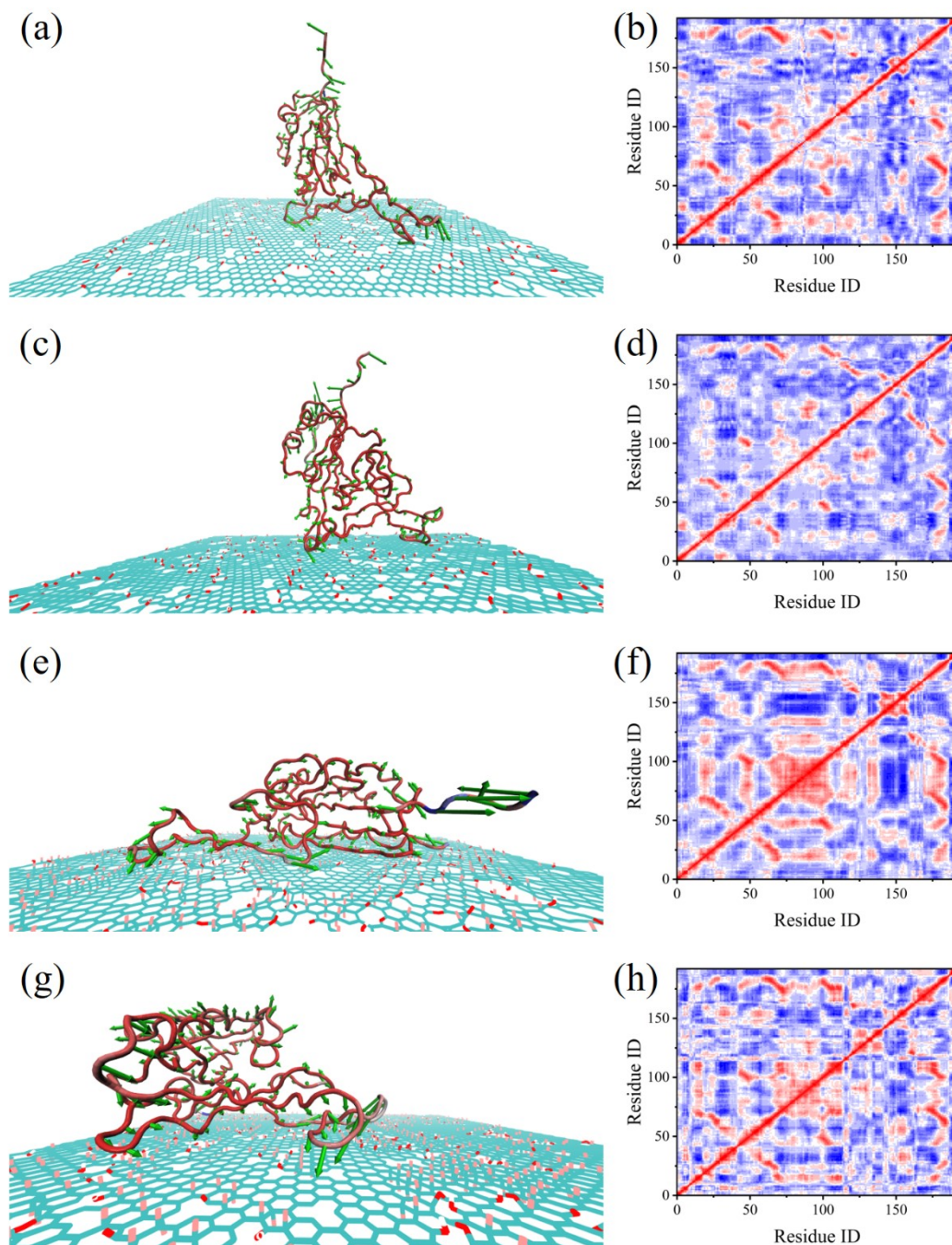


Fig. S22. At 500 ns, hedgehog plot and DCCM of RBD, which adsorbed on the (a-b, e-f) DG and (c-d, g-h) FDG. Investigated materials highlighted by “Lines” drawing methods. The C, O, H and F atoms of investigated materials are represented by cyan, red, white and pink balls, respectively.

Color scale: Dark Blue (-0.88) - Dark Red (1).

21. Hedgehog plot and DCCM of M^{pro}

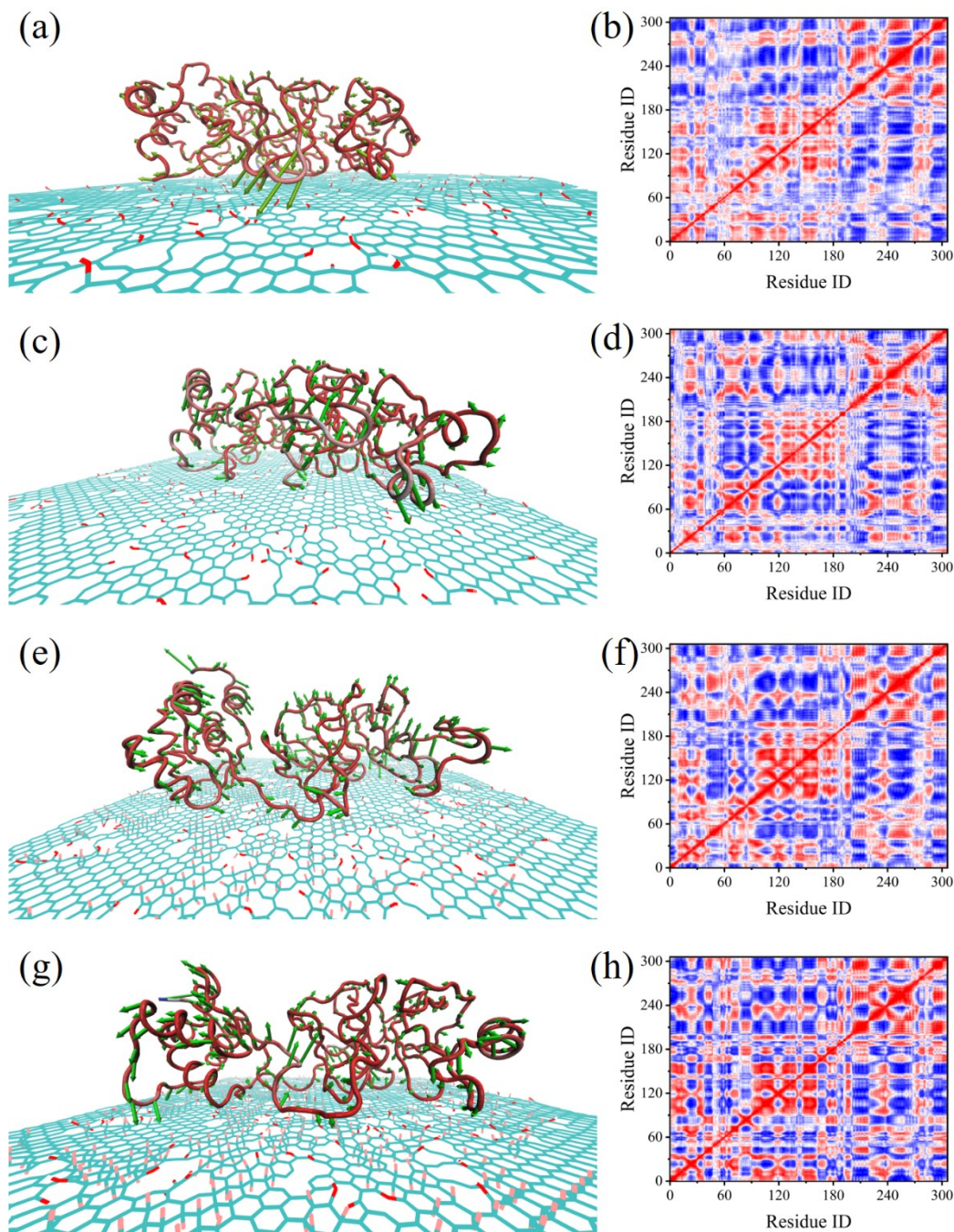


Fig. S23. At 500 ns, hedgehog plot and DCCM of M^{pro}, which adsorbed on the (a-b, e-f) DG and (c-d, g-h) FDG. Investigated materials highlighted by “Lines” drawing methods. The C, O, H and F atoms of investigated materials are represented by cyan, red, white and pink balls, respectively.

Color scale: Dark Blue (-0.88) - Dark Red (1).

22. The interaction energy between small peptide and the FDG

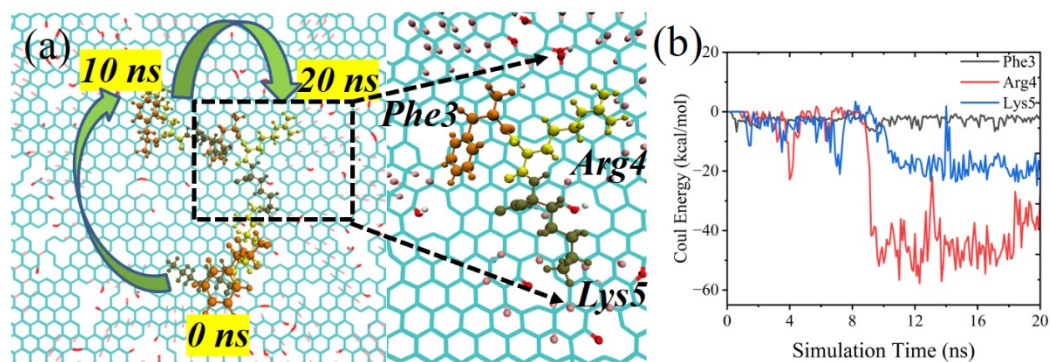


Fig. S24. (a) The migration process of small peptides on the FDG. (b) The Coulomb energy curve between amino acids and FDG during migration process. Amino acids and investigated materials highlighted by “CPK” and “Lines” drawing methods. The C, O, H and F atoms of investigated materials are represented by cyan, red, white and pink balls, respectively.

23. Path of deoxynucleotides relative to investigated materials

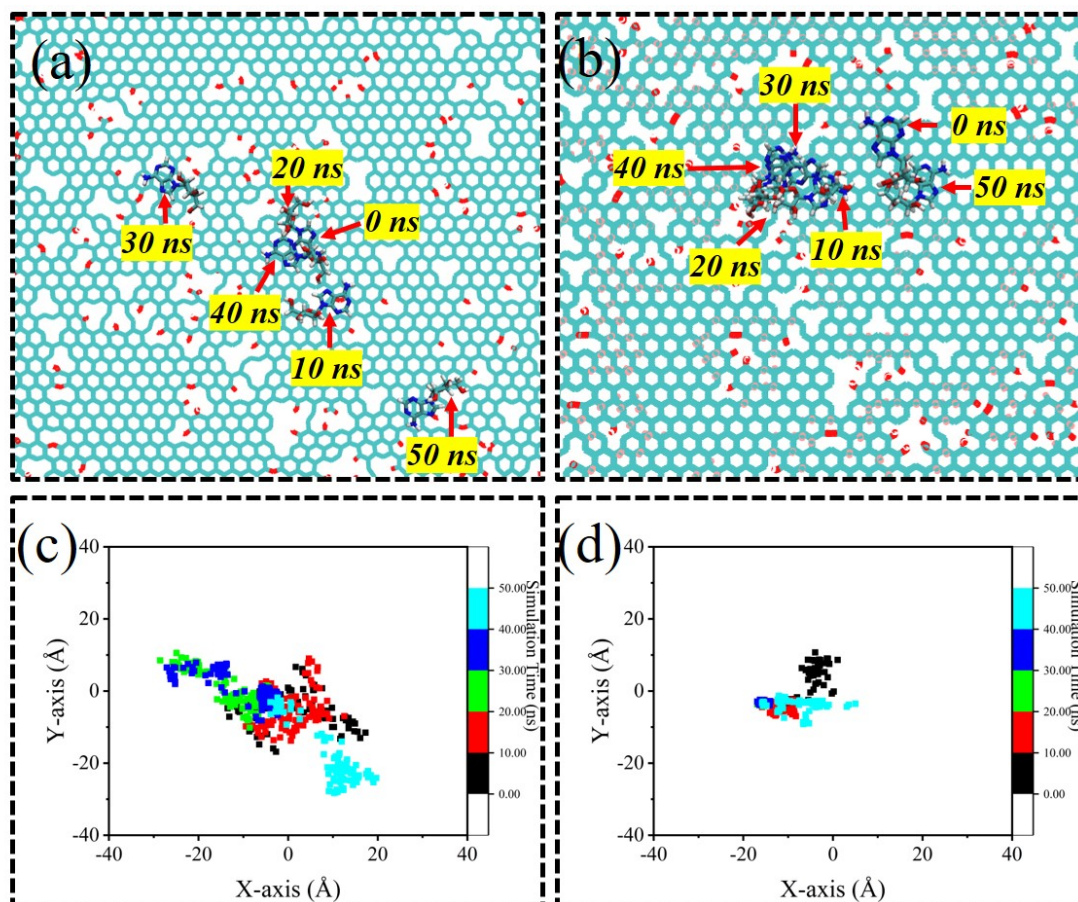


Fig. S25. Representative snapshot and migration path of deoxyadenosine monophosphate (dAMP) on the (a, c) DG and (b, d) FDG. dAMP and investigated materials highlighted by “Licorice” and “Lines” drawing methods. The C, O, H and F atoms of investigated materials are represented by cyan, red, white and pink balls, respectively.

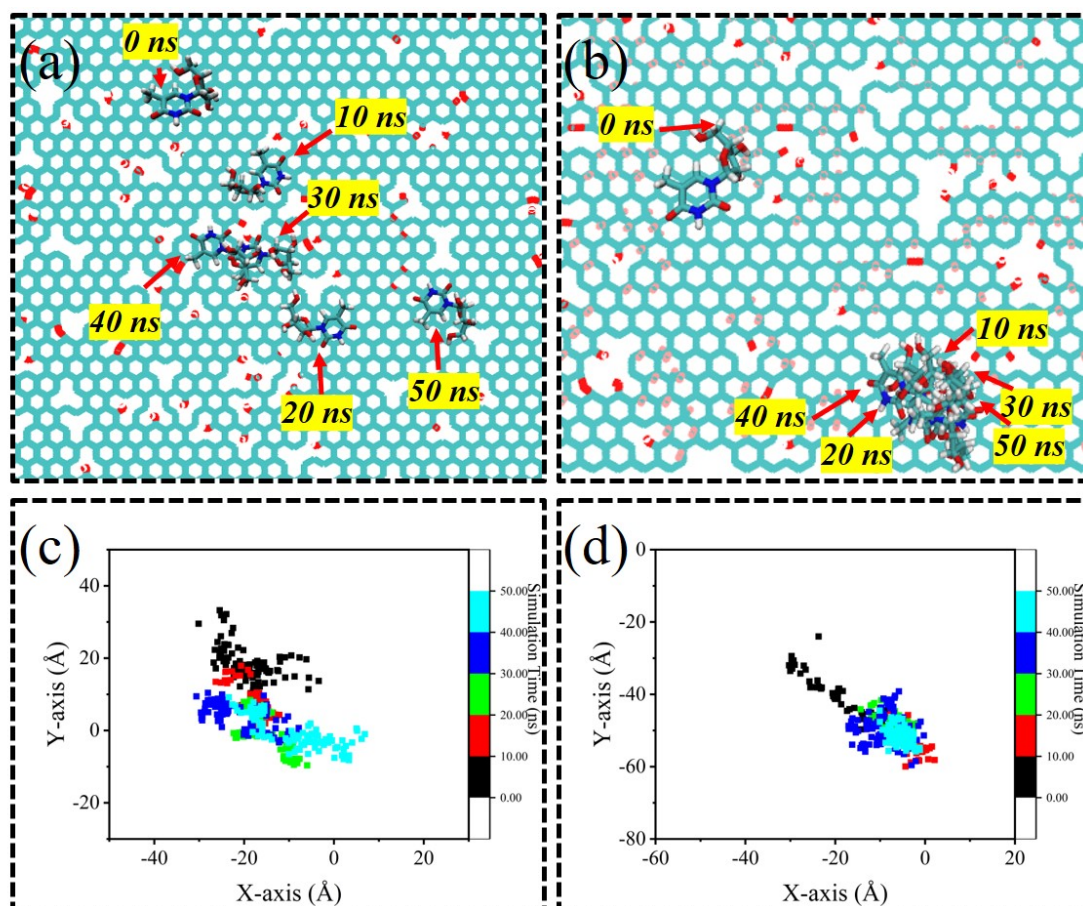


Fig. S26. Representative snapshot and migration path of deoxythymidine monophosphate (dTMP) on the (a, c) DG and (b, d) FDG. dTMP and investigated materials highlighted by “Licorice” and “Lines” drawing methods. The C, O, H and F atoms of investigated materials are represented by cyan, red, white and pink balls, respectively.

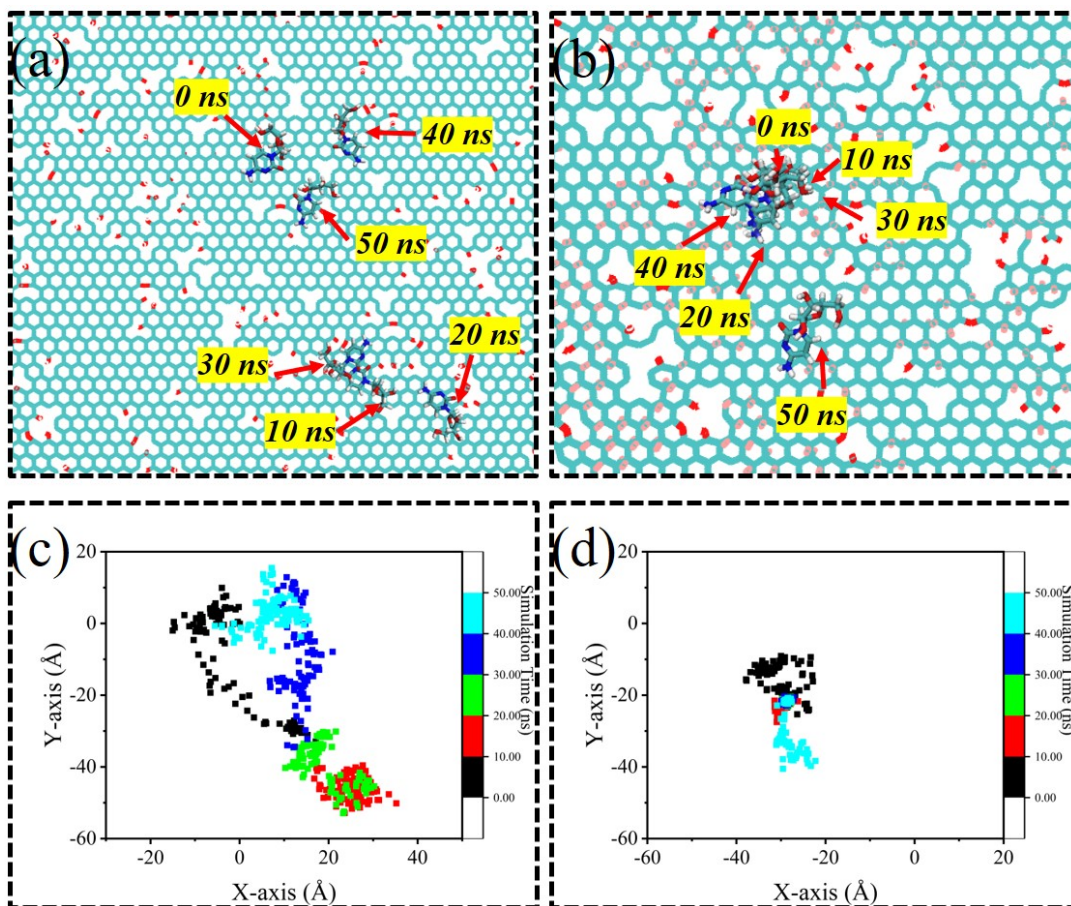


Fig. S27. Representative snapshot and migration path of deoxycytidine monophosphate (dCMP) on the (a, c) DG and (b, d) FDG. dCMP and investigated materials highlighted by “Licorice” and “Lines” drawing methods. The C, O, H and F atoms of investigated materials are represented by cyan, red, white and pink balls, respectively.

References

1. D. Zhao, L. Li, D. He and J. Zhou, *Applied Surface Science*, 2016, **377**, 324-334.